

Transduction of temporal patterns by single neurons

Scott L. Hooper

Neurobiology Program, Department of Biological Sciences, Ohio University, Athens, Ohio 45701, USA

Correspondence should be addressed to S.L.H. (Hooper@ohiou.edu)

As our ability to communicate by Morse code illustrates, nervous systems can produce motor outputs, and identify sensory inputs, based on temporal patterning alone. Although this ability is central to a wide range of sensory and motor tasks, the ways in which nervous systems represent temporal patterns are not well understood. I show here that individual neurons of the lobster pyloric network can integrate rhythmic patterned input over the long times (hundreds of milliseconds) characteristic of many behaviorally relevant patterns, and that their firing delays vary as a graded function of the pattern's temporal character. These neurons directly transduce temporal patterns into a neural code, and constitute a novel biological substrate for temporal pattern detection and production. The combined activities of several such neurons can encode simple rhythmic patterns, and I provide a model illustrating how this could be achieved.

We effortlessly identify sensory inputs on the basis of temporal patterning alone (for instance, different Morse code symbols) and as effortlessly produce motor outputs with widely differing temporal patterning (slow versus fast walking, walking versus skipping). This ease belies what is, *a priori*, a difficult task for nervous systems. Indeed, despite its central importance in speech comprehension and music appreciation, and in producing behaviorally relevant motor output, the neurobiological bases of temporal pattern interpretation, and the control of temporal pattern production, remain poorly understood.

To appreciate the difficulty of these tasks, consider four temporal patterns (Fig. 1; this example is couched in terms of pattern interpretation, but analogous difficulties exist for pattern production). In each panel, time proceeds from left to right, and the signal (for instance, a tone) is on in the up, and off in the down, portion of the trace. These patterns have a number of similarities. Patterns 1 and 4 have equal tone durations but different intertone intervals. Patterns 2 and 3 have equal intertone intervals but different tone durations. Patterns 1 and 3 have the same repeat time (cycle period, equal to tone duration plus intertone interval), but differ in all other parameters, and are thus different rhythms played at the same speed. Patterns 1 and 2 (and patterns 3 and 4) have the same duty cycle (the proportion of a cycle in which the tone is on; 50% and 75% respectively) but different cycle periods, and are thus the same rhythm played at different speeds.

Two hypotheses have been advanced to explain our ability to recognize similarities and differences between these patterns. The first is that nervous systems distinguish temporal patterns by measuring on and off durations¹⁻⁴. However, many patterns have on and off durations in the hundreds of milliseconds, and how nervous systems could measure such long times is unclear. This hypothesis also requires that earlier and later durations be stored and compared (for example, distinguishing among patterns 1-4 would require comparing successive tone durations and intertone intervals)⁵, and how nervous systems would perform this task is unknown. Furthermore, under this hypothesis, our ability to identify patterns on the basis of relative timing (that is,

knowing that 1 and 2 are the same pattern at different speeds) requires dividing tone duration by cycle period, and how nervous systems would make this calculation is also unknown.

Another hypothesis is that nervous systems distinguish temporal patterns using a distributed neural network, in which each pattern induces activity in a unique set of neurons^{2,6}. However, each pattern would activate an arbitrary set of neurons, and this scheme thus provides no mechanism to identify pattern similarity (that 1 and 2 have the same duty cycle, and 1 and 3 the same period), and again this hypothesis lacks experimental evidence. Finally, neither hypothesis explains the psychophysical observation that sensory processing and motor pattern production show certain temporal similarities, which have been interpreted as suggesting that they share a common timing mechanism^{4,7}.

I propose here a hypothesis that obviates these difficulties. Distinguishing among the patterns in Fig. 1 requires a site in the nervous system in which two pattern parameters are compared. For instance, comparing tone duration and intertone interval distinguishes each pattern because 1, 2 and 3 have different durations, and 1 and 4 different intervals. Identifying similarity requires a site in the nervous system whose activity does not change if the similarity criterion does not change; for example, if the criterion is duty cycle, there should be a site whose activity is the same for patterns 1 and 2, even though the tone durations, intertone intervals and periods of these patterns all differ.

Consider a neuron that fires when the tone in Fig. 1 is on, but is otherwise silent. If the neuron has conductances whose activation and inactivation are voltage-dependent and slow in comparison to rhythm period, the average activation of these conductances would be expected to vary as a function of both tone duration and intertone interval⁸, as also might the neuron's average calcium and calcium-dependent second-messenger concentrations⁹. The neuron's activity during the tone might thus vary as a graded function of the recent history (that is, the previous few cycles) of both tone duration and intertone interval—for example, its firing frequency might equal $5 \times \text{duration} + 15 \times \text{interval}$ —and hence provide a locus whose activity depends

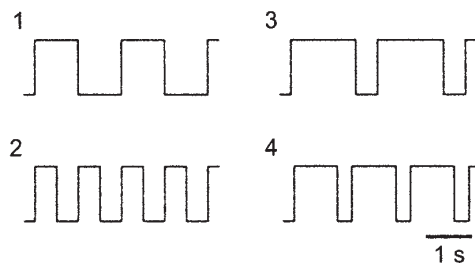


Fig. 1. Four rhythmic patterns. 1 and 2, and 3 and 4, have the same duty cycles, but different cycle periods; 1 and 3 have the same period.

on two pattern parameters. Such a neuron would also automatically do a type of similarity sorting, because it would fire at the same frequency for all patterns that had a certain relationship between their elements. For instance, this neuron would fire at 10 Hz for all patterns in which duration = 2 seconds – $3 \times$ interval. It would thus fire at 10 Hz for a pattern with 0.1-second interval and 1.7-second duration, or with 0.2-second interval and 1.4-second duration, or 0.3-second interval and 1.1-second duration, and so on. Similarly, it would fire at 20 Hz for all patterns in which duration = 4 seconds – $3 \times$ interval (for example, patterns with interval of 0.1, duration of 3.7; interval of 0.2, duration of 3.4; interval of 0.3, duration of 3.1, etc.).

Such 'pattern-sensitive' neurons would be analogous to primary afferent neurons in that they would directly transduce temporal pattern relationships into a neural code. This hypothesis overcomes all the drawbacks noted above. First, because pattern-sensitive neurons respond directly to pattern relationships, no explicit knowledge of time is required. Second, because the neuron's response is a graded function of pattern, changes in neuron activity directly correlate with pattern changes. Third, comparison of the output of neurons with different dependencies can identify different patterns (see Discussion). Fourth, such neurons automatically sort patterns by similarity. Fifth, the presence of such neurons in both sensory and motor networks could explain the similarity in sensory and motor temporal processing that has been observed psychophysically.

Here I present experimental evidence for neurons that respond to specific features of temporal patterns, and show that such neurons could be used to distinguish among simple rhythms. Such neurons may have a key role in rhythmic pattern production and interpretation.

Results

I have been investigating these issues in the rhythmic pyloric network of the lobster, *Panulirus interruptus*. Rhythmic patterns are advantageous because of their behavioral relevance (many auditory, and most locomotory, patterns are rhythmic), because animals express many rhythmic patterns (mating versus warning calls, walking versus running), because most rhythmic patterns can be produced in a variety of ways (slow versus fast talking) and because rhythmic patterns are easy to define (see Fig. 1). The pyloric network is advantageous because the network produces a variety of patterns, each across a wide range of cycle periods, *in vivo*¹⁰;

network output and period can be experimentally altered *in vitro*^{11–28}; the network's synaptic connectivity^{29,30} and many of the intrinsic properties of its neurons^{8,31–37} are known; and pyloric neurons can be isolated from the network^{38,39}. The pyloric pattern is typically defined by cycle period and duty cycle (rather than burst duration and interburst interval), and I therefore use these parameters here (because period = duration + interval and duty cycle = duration/period, these descriptions are equivalent). I report here that some pyloric neurons respond to rhythmic input with intrinsic responses that are graded functions of the recent history of these parameters.

In the pyloric network (Fig. 2a), the network's pacemaker ensemble, consisting of the Anterior Burster (AB) and Pyloric Dilator (PD) neurons, inhibits all other neurons within the network. These latter neurons fire after inhibition because hyperpolarization induces post-inhibitory rebound and a sustained 'plateau'³¹; their firing order, burst durations and interburst delays are determined by the network's synaptic connectivity and by the intrinsic dynamics of the individual neurons^{32,40}. This combination of synaptic connectivity and neuronal properties results in a pattern in which the AB and PD neurons fire first, followed by the Lateral Pyloric (LP) and Inferior Cardiac (IC) neurons, and finally by the Ventricular Dilator (VD) and the six to eight Pyloric (PY) neurons, after which the pattern repeats (Fig. 2b).

Of particular importance here are the delays between the burst endings of the neurons (such as the PD neuron, PD_{end}) that inhibit the PY neurons, and the PY neuron burst beginnings (PY_{begin}), and in particular how these delays change with cycle period. I therefore altered pyloric period by tonic current injection into the network's pacemaker AB neuron. In all cases, these delays increased with cycle period²⁸. I show here data for one such delay (from PD_{end} to PY_{begin}; Fig. 3). Note that the effects are large; delay increases by ~0.45 seconds as period increases from 0.4 to 2 seconds. (For a detailed analysis of pyloric phase as period is altered, see refs 27, 28.)

The PY neurons are a heterogeneous group³⁴, and because the PY response is recorded extracellularly from a population

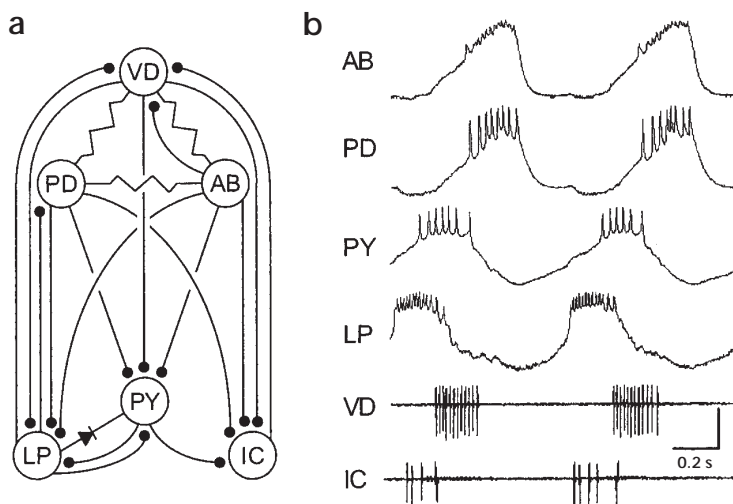


Fig. 2. The pyloric network and rhythm. (a) Schematic of the network's synaptic connectivity. Closed circles represent inhibitory synaptic connections, resistor symbols electrical coupling, the diode a rectifying electrical synapse. (b) The rhythm consists of a pattern in which first the AB and PD, then the LP and IC, and finally the PY and VD neurons burst, after which the pattern repeats. Vertical scale bar, 14 mV for PD and PY neurons, 7 mV for the others.

of neurons, these delay changes could reflect the recruitment of different types of PY neurons at different network cycle periods. This is not the case, however; intracellular recordings (data not shown) demonstrate that the same PY neurons remain active, and that most PY neurons show similar delay changes, as network cycle period is altered. Ending–beginning delays arise from a combination of the decreasing of the synaptic inhibition and the delay of the intrinsic rebound response of the PY neuron. The observed shifts in delay could thus arise from changes in inhibition time course, PY neuron rebound delay, or both. To determine whether there is a change in the intrinsic delay of the PY neuron rebound, I isolated PY neurons from the network by photoinactivating and pharmacologically blocking their presynaptic inputs. Isolated PY neurons are spontaneously silent or show slow tonic firing, but rhythmic hyperpolarizing current pulses injected into the cell body cause them to fire robustly because of post-inhibitory rebound.

Isolated PY neurons were therefore impaled with two electrodes (one to inject current, the other to measure activity), and their rebound delay was measured during rhythmic current pulse trains with various cycle periods and duty cycles. (The pyloric network also produces patterns with a variety of duty cycles^{10–26}.) All isolated PY neurons ($n = 7$ cells, 5 preparations) fulfilled one requirement of the proposed hypothesis, in that a neuronal activity characteristic (rebound delay) depended in a graded fashion on two parameters that define the temporal pattern (cycle period and duty cycle). In an isolated PY neuron given pulse trains with a 0.5 duty cycle and periods of either 0.5 or 2.1 seconds, rebound delay increased linearly (from ~ 0.2 to ~ 0.36 s) as period increased (Fig. 4a). In another isolated PY neuron given pulses with a period of 1 second and duty cycles of 0.33 or 0.67, rebound delay increased linearly (from ~ 0.23 to ~ 0.39 s) as duty cycle increased (Fig. 4b). The rebound delays of another isolated PY neuron in

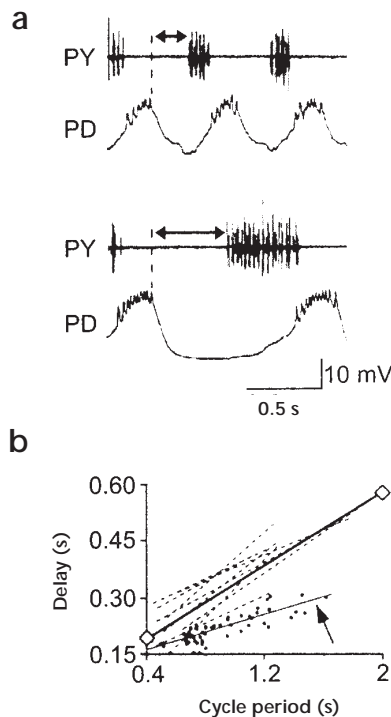


Fig. 3. Pyloric interneuronal delays shift as cycle period is altered. **(a)** When pyloric period increases, the delay from PD neuron burst ending to PY neuron burst beginning (double-headed arrows) increases. PY, extracellular PY neuron recording; PD, intracellular PD neuron recording. **(b)** Summary plot. PD to PY delay increases ~ 0.45 seconds as period increases from 0.4 to 2 seconds. Closed circles, data from one preparation; dashed lines, fits to individual experiments; coarse lines with diamonds, average of all experiments.

response to rhythmic trains with a wide range of cycle periods and duty cycles could be fitted well to a plane (Fig. 4c; $R = 0.89$). Similar results were obtained from every isolated PY neuron, although each neuron's period- and duty-cycle-dependence (the intercepts and slopes of the fits) was different, even among neurons in a single preparation (Table 1; all regressions were significant at $p < 0.001$).

The second requirement of the proposed hypothesis is that neuronal activity must change rapidly as the pattern changes, because pattern-sensitive neurons would have little utility if they took hundreds of cycle periods to respond to pattern changes. The period of the pyloric cycle varies from 0.5 to 2.0 seconds, so a PY neuron that averages over the past two to three seconds would be sufficient to respond to the entire range. An isolated PY neuron at the onset of a train of pulses with a period of 1 second and a duty cycle of 0.33 (Fig. 5) fired tonically before the first pulse.

During the first interpulse interval, the rate of depolarization was sufficiently slow relative to the pulse duration that the neuron did not fire. (Longer pulses, data not shown, confirmed that during this first interval, the rebound delay was longer than the duration of the pulses used here.) By the second interpulse interval, the rebound delay had shortened enough that the neuron fired a single spike, and by the third interval, rebound delay had stabilized. Similar rapid stabilization was found at all (~ 350) pattern changes that were used to generate the present data.

Discussion

It is important to contrast these data to earlier work in which pyloric neuron activity was also altered by temporally varying inputs^{41–44}. This work showed that long-

Table 1. PY neuron preparation number, regression equation and correlation coefficient.

Preparation number	Regression equation	Correlation coefficient
1	$-0.06 + 0.08 \times \text{period} + 0.61 \times \text{duty cycle}$	0.91
2 (Fig. 6 neuron B)	$0.02 + 0.06 \times \text{period} + 0.34 \times \text{duty cycle}$	0.93
2 (Fig. 4b)	$-0.14 + 0.13 \times \text{period} + 0.59 \times \text{duty cycle}$	0.90
3 (Fig. 4a; Fig. 6 neuron A)	$-0.09 + 0.07 \times \text{period} + 0.48 \times \text{duty cycle}$	0.77
3 (Fig. 6 neuron C)	$0 + 0.01 \times \text{period} + 0.36 \times \text{duty cycle}$	0.92
4	$-0.4 + 0.3 \times \text{period} + 1.01 \times \text{duty cycle}$	0.88
5 (Fig. 4c)	$-0.05 + 0.04 \times \text{period} + 0.44 \times \text{duty cycle}$	0.89

The data are from seven PY neurons from five preparations. Column 1 indicates which neurons are illustrated in which figures. Column 2 shows the two-dimensional regression equation of rebound delay for each neuron; note that each equation (even those of neurons from the same preparation) has different intercepts and slopes. Column 3 shows the correlation coefficient (R) for each regression.

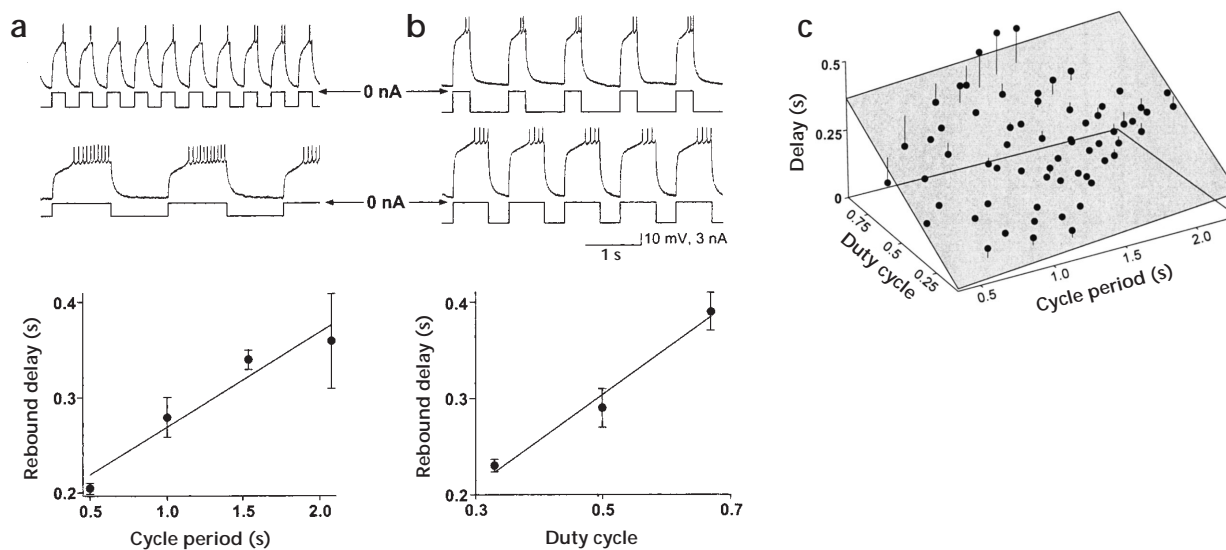


Fig. 4. Isolated PY neuron rebound delay depends on cycle period and duty cycle. **(a)** Rebound delay increases when inhibitory pulse train period increases. Top panel, 50% duty-cycle stimulus trains at periods of 0.5 seconds (top trace, intracellular PY neuron recording; next trace, current monitor) and 2.1 seconds (bottom two traces). Bottom panel, summary plot. **(b)** Rebound delay increases with increasing duty cycle. Top panel, one-second period trains at duty cycles of 0.33 (top two traces) and 0.67 (bottom two traces). Bottom panel, summary plot. **(c)** Isolated PY neuron rebound delay is a linear function of period and duty cycle. PY neuron rebound delays in response to stimulation trains with a variety of periods and duty cycles. The slanted plane is a two-dimensional linear regression; the lines dropped from the data points to the plane represent the vertical (z) distance of the points from the plane. For data points without lines, the distance from the plane is less than the point's diameter.

term alterations of neuronal conditions (isolation in cell culture, hour-long stimulations) resulted in compensatory homeostatic changes that drove the neurons toward their control activity. These changes, however, are probably too slow to generate or detect short-term changes in temporal patterning. The present work, in contrast, tested how neurons respond to the short-term variations typical of everyday sensory and motor patterns and was therefore done with short stimulation protocols (~30 s). In these experiments, the rebound delays of PY neurons showed no sign of long-term compensatory changes. Instead, delay rapidly assumed the value appropriate for the input pattern and maintained this value so long as the input did not change.

The effect of cycle period on rebound delay in isolated PY neurons raises the question of whether this property is involved in maintaining their timing in the intact network (see Fig. 3).

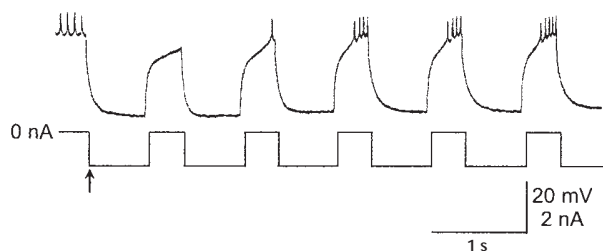


Fig. 5. PY neuron rebound delays stabilize rapidly. The neuron fired tonically before the onset (arrow) of the stimulus train. The first interpulse interval was shorter than the rebound delay, and the neuron did not fire. Rebound delay had shortened sufficiently for a single spike by the second interpulse interval and had stabilized by the third.

The shifts in rebound delay found in isolated PY neurons are approximately half the size of those observed in the intact network (compare Figs 3b and 4a, bottom left panel). Thus, although these shifts are presumably involved in maintaining PY neuron phase in the network, they are unlikely to be solely responsible. Different PY neurons show different dependencies of rebound delay on period and duty cycle; this may reflect their functional heterogeneity, in that different classes of PY neurons have different postsynaptic targets within the pyloric network³⁴ and innervate different pyloric muscles⁴⁵. These different dependencies could thus help shape pyloric network activity as cycle period changes, or they could be required for appropriate pyloric movements as period changes, or both.

PY neuron rebound delay arises in part from the transient potassium current I_A (ref. 34), and pharmacologically induced variation of I_A can lead to shifts in the rebound delay of isolated PY neurons³⁷. It is thus natural to expect that the rebound delay variations reported here might arise from a dependence of I_A on cycle period and duty cycle. I have not measured I_A , but we were unable to reproduce the period and duty-cycle dependence reported here in a series of computer simulations (A.L. Weaver, R.A. DiCaprio & S.L.H. *Soc. Neurosci. Abst.* 22, 131, 1996) using existing PY neuron models³⁷ in which the parameters governing I_A (and I_h) were varied over a wide range. Although this work cannot prove that no I_A and I_h parameter set would give rise to this dependence, it does raise the possibility that additional currents are involved in this process.

Pattern-sensitive neurons respond to the pattern as a whole, and thus they would seem ideally suited to serve as building blocks for temporal pattern interpretation and production. As noted earlier, pattern-sensitive neurons divide patterns into classes based on the relationship between pattern parameters. For

instance, if a neuron's rebound delay equals $c + a \times \text{period} + b \times \text{duty cycle}$, the neuron will have a given rebound delay D for all patterns in which $\text{duty cycle} = (D - c - a \times \text{period})/b$. Although this similarity sorting is robust (all patterns with this relationship will give the same delay, and this delay will occur only with patterns that have this relationship), clearly an infinite number of duty cycle/period pairs satisfy this equation. This confounding of two pattern parameters by pattern-sensitive neurons means that individually these neurons cannot identify either parameter; how then could such neurons be used to uniquely identify patterns? Theoretically, comparing two such neuron's outputs would suffice, because solving $\text{del}_A = c_1 + a_1 \times \text{period} + b_1 \times \text{duty cycle}$ and $\text{del}_B = c_2 + a_2 \times \text{period} + b_2 \times \text{duty cycle}$ simultaneously gives $\text{period} = (b_1(c_2 - \text{del}_B) + b_2(\text{del}_A - c_1))/(a_1b_2 - a_2b_1)$ and $\text{duty cycle} = (a_1(\text{del}_B - c_2) + a_2(c_1 - \text{del}_A))/(a_1b_2 - a_2b_1)$. However, this requires explicit knowledge of rebound delay ($\text{del}_A, \text{del}_B$), which can be as large as 500–600 ms. As noted earlier, it is unclear how nervous systems could track such long times.

An alternative method that obviates the need to track long times is to use a coincidence detector based on delay lines (Fig. 6). Because such detectors compare the time difference between events, most of the rebound delay would be subtracted out. To make this concrete, consider the rebound delay (z axis) versus period (x axis) and duty cycle (y axis) regression planes for three actual PY neurons (bottom panels). All three neurons show a large rebound-delay range (the z axis is from 0 to 0.75 s), and the fit for each neuron has a different intercept and slope.

The model consists of a two-dimensional array of coincidence-detector neurons, each of which receives appropriately delayed input from all three PY neurons. All the neurons in a column receive spikes from neurons A (black) and B (blue) with the delay-line delays shown under the column. For instance, neuron A is connected to each neuron in the left-most column with a delay line of 0.051 seconds, meaning that neurons in this column receive input from neuron A 0.051 seconds after it fires. Neuron B is connected to each neuron in the same column with a delay line of 0.04 seconds, and these neurons thus receive input from neuron B 0.04 seconds after it fires. Each neuron in this column therefore receives coincident input when neuron A fires $0.051 - 0.04 = 0.011$ seconds before neuron B. To appreciate the subtractive nature of coincidence detection through delay lines, consider a pattern with a period of 1.5 seconds and a duty cycle of 0.6. The rebound delays of neurons A and B to this pattern are very large (0.303 and 0.314 s). The difference between these rebound delays is 0.011 seconds, and all the neurons in the left-most column therefore receive coincident input when this pattern is played. Because the detector senses the difference between rebound delays, rather than their (much larger) absolute values, this detection is accomplished using delay lines of only 0.051 and 0.04 seconds.

This process is equivalent to subtracting the equation for neuron A, $z = -0.09 + 0.07x + 0.48y$, from that of neuron B, $z = 0.02 + 0.06x + 0.34y$, and setting the result equal to 0.011; all the neurons in this column thus receive coincident input for all patterns in which $0.011 = 0.11 - 0.01 \times \text{period} - 0.14 \times \text{duty cycle}$. An infinite number of period/duty cycle pairs will satisfy this equation, and so two neurons cannot uniquely specify period and duty cycle when their rebound delay differences are compared. The ambiguity can be resolved, however, by having the coincidence detector neurons also receive appropriately delayed input from a third neuron, C. All the neurons in each row of the detector receive neuron C input with the delay noted at the right of the row. For example, all the neurons in the detector's bottom row

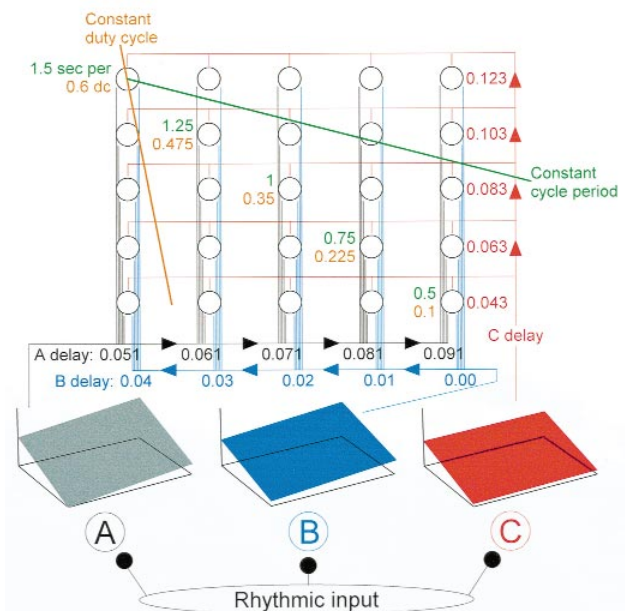


Fig. 6. Coincidence detection among three pattern-sensitive neurons can be used to identify simple rhythmic patterns. Bottom panels, planar regressions of three isolated PY neurons; neurons A and C are from the same preparation. x axes, period (0.3 to 2.3 s); y axes, duty cycle (0.1 to 0.9); z axes, rebound delay (0 to 0.75 s). Note that the three planes have different intercepts and slopes. Top panel, a coincidence detector that uses the differences between the rebound delays of these neurons to uniquely code the period and duty cycle of their rhythmic inputs. See text for full description.

receive neuron C input with a 0.043-second delay, all the neurons in the next row up receive neuron C input with a 0.063-second delay, and so on. (The appropriate delays were obtained by considering $A - C = -0.09 + 0.06 \times \text{period} + 0.12 \times \text{duty cycle}$.)

As a result of these delay lines, each detector neuron receives coincident input from all three receptor neurons at only one period and duty cycle. For instance, if period and duty cycle are 1.5 seconds and 0.6, the rebound delays of neurons A, B and C are 0.303, 0.314 and 0.231 seconds. The neuron labeled '1.5 s per 0.6 dc' therefore receives neuron A input at the sum of neuron A's rebound delay—0.303 seconds—and neuron A's delay-line delay—0.051 seconds—and thus receives input from neuron A $0.303 + 0.051 = 0.354$ seconds after the end of each hyperpolarizing pulse in the pattern. Similarly, this neuron receives neuron B input 0.314 (neuron B's rebound delay) + 0.04 (neuron B's delay-line delay) = 0.354 seconds after the end of each pulse, and neuron C input 0.231 (neurons C's rebound delay) + 0.123 (neuron C's delay-line delay) = 0.354 seconds after the end of each pulse. If each detector neuron requires coincident input from neurons A, B and C to fire, then its activity uniquely specifies one period and duty cycle. Numbers next to the neurons on the detector diagonal are the cycle period (green) and duty cycle (orange) of the pattern those neurons sense. The green line marks the detector positions for a constant period of 1.5 seconds (only duty cycle varies along this line). Thus, a higher-order neuron that fired when any detector neuron positioned on this line was active would fire for all patterns with a period of 1.5 seconds regardless of their duty cycle. Such higher-order neurons that received input from iso-

frequency lines in the coincidence detector would thus sort patterns by period. The orange line marks the detector positions for a constant duty cycle of 0.6 (only period varies along this line). Thus, a higher-order neuron that fired when any detector neuron positioned on this line was active would fire for all patterns with a duty cycle of 0.6 regardless of their period. Such higher-order neurons that received input from iso-duty cycle lines in the coincidence detector would thus sort patterns by duty cycle.

There are two points to make about this figure. First, although the delay lines are much shorter than the rebound delays, they are still too large to implement with a single axonal delay line⁴⁶. However, the compression degree depends only on the slope and intercept differences of the planes being compared; more similar planes would require shorter delays. (The PY neurons, after all, did not evolve to drive a coincidence detector, but instead to function in the relatively slow pyloric network, in which large delay differences may be necessary to achieve appropriate responses in their postsynaptic targets.) Second, this figure is primarily intended to illustrate how pattern-sensitive neurons could be used to uniquely identify different patterns, and I am not suggesting that its exact implementation will be found in real nervous systems. In particular, the coincidence detector shown here will only work after the pattern-sensitive neurons have reached steady state (see Fig. 5), and thus this scheme will not work during transitions between patterns, or for irregular patterns. Nonetheless, the relative ease and neurobiological plausibility of its construction clearly shows the potential utility of pattern-sensitive neurons for the production and analysis of temporal patterns.

In summary, the PY neurons of the lobster pyloric network change their rebound delay as a graded function of the recent history of two pattern parameters, cycle period and duty cycle. These neurons directly transduce pattern into a neural code without explicit time measurement or network-based computation and can therefore be considered pattern-sensitive neurons. Comparison of the output of such neurons can uniquely identify different rhythmic patterns, and such neurons could be a key neurobiological substrate for the production and identification of different rhythms.

Methods

All techniques were standard. Extracellular recordings were made with stainless-steel pin electrodes and an A-M Systems differential amplifier. Intracellular recordings and current injection were made with glass microelectrodes filled with 0.55 M K₂SO₄, 0.02 M KCl (resistance 10 to 20 MΩ) and an Axoclamp 2A. Signals were displayed on an Astro-Med MT9500 electrostatic chart recorder and recorded on a Microdata DT-800 digital tape recorder. Cycle period was altered by current injection into the AB neuron. In all experiments, the stomatogastric nerve, which carries input from the rest of the lobster nervous system to the pyloric network, was kept intact. PY neurons were isolated from the network by photoinactivating the PD and VD neurons and blocking remaining network synaptic input with picrotoxin^{38,39}. All experiments were done with two electrodes in the neurons, one for voltage recording, the other for current injection. Small (< 1 nA) depolarizing or hyperpolarizing tonic current was injected into two of the neurons to bring them near threshold; the other neurons were near threshold at rest, and no background current was injected. Average membrane potential of the neurons before pulse-train stimulation (holding potential for the two into which tonic current was injected, rest for the others) was -46 ± 6 mV.

In the intact network, the most hyperpolarized voltage achieved by the PY neurons is (depending on the preparation) between -55 and -70 mV, and varies only slightly (< 5 mV) as cycle period is altered by current injection into the AB neuron. The dependence of isolated PY neuron rebound delay on cycle period and duty cycle shown here is present for

current injections of all amplitudes sufficient to reliably induce post-inhibitory rebound. However, the magnitude of the rebound delays progressively increases as current-pulse amplitude increases (i.e., the planes in Figs 4c and 6 shift upward) until the membrane potential achieved during the current pulse is more negative than ~ -70 mV. At this point, PY neuron rebound delay ceases to depend on membrane potential (data not shown); all data presented here were obtained with current pulses of this amplitude or larger. Stimulus trains were generated using a Grass Instruments S48 stimulator and World Precision Instruments stimulus isolation unit. Data were analyzed using Spike II scripts after transfer (Cambridge Electronic Design 1401 laboratory interface) to a Gateway 2000 P5. PY neuron rebound delay data points are averages of at least 10 pulses after delay stabilized. Plots were generated using Kaleidagraph (Synergy Software) and Axum (Mathsoft) plotting and Canvas (Deneba) drawing software. Axum cannot plot error bars on three-dimensional plots; standard deviations on these plots varied between 0 and 0.03 seconds, with larger deviations being associated with larger delays. Linear fit *R* values were calculated using Kaleidagraph; planar fit *R* values with SPSS statistical software.

Acknowledgements

I thank R. A. DiCaprio, L. G. Morris and A. L. Weaver for reading the manuscript, discussion and advice, J. B. Thuma for technical assistance and H. L. Atwood for the donation of micromanipulators. This research was supported by grants from the National Science Foundation, the Human Frontier Science Program and Ohio University and its research council.

RECEIVED 10 AUGUST; ACCEPTED 27 OCTOBER 1998

1. Treisman, M. Temporal discrimination and the indifference interval: implications for a model of the 'internal clock'. *Psychol. Monographs* 77, 1–31 (1963).
2. Ivry, R. B. The representation of temporal information in perception and motor control. *Curr. Opin. Neurobiol.* 6, 851–857 (1996).
3. Treisman, M., Faulkner, A., Naish, P. L. N. & Brogan, D. The internal clock: evidence for a temporal oscillator underlying time perception with some estimates of its characteristic frequency. *Perception* 19, 705–743 (1990).
4. Treisman, M., Faulkner, A. & Naish, P. L. N. On the relation between time perception and the timing of motor action: evidence for a temporal oscillator controlling the timing of movement. *Q. J. Exp. Psychol.* 45, 235–263 (1992).
5. Wang, D. in *The Handbook of Brain Theory and Neural Networks* (ed Arbib, M. A.) 967–971 (MIT Press, Cambridge, MA, 1995).
6. Buonomano, D. V. & Merzenich, M. M. Temporal information transformed into a spatial code by a neural network with realistic properties. *Science* 267, 1028–1030 (1995).
7. Ivry, R. B. & Hazeltine, R. E. The perception and production of temporal intervals across a range of durations: evidence for a common timing mechanism. *J. Exp. Psychol. Hum. Percept. Perform.* 21, 1–12 (1995).
8. Abbott, L. F., Marder, E. & Hooper, S. L. Oscillating networks: control of burst duration by electrically coupled neurons. *Neural Computation* 3, 487–497 (1991).
9. De Koninck, P. & Schulman, H. Sensitivity of CaM kinase II to the frequency of Ca²⁺ oscillations. *Science* 279, 227–230 (1998).
10. Rezer, E. & Moulins, M. Expression of the crustacean pyloric pattern generator in the intact animal. *J. Comp. Physiol. A* 153, 17–28 (1983).
11. Sigvardt, K. A. & Mulloney, B. Properties of synapses made by IVN command-interneurons in the stomatogastric ganglion of the spiny lobster *Panulirus interruptus*. *J. Exp. Biol.* 97, 153–168 (1982).
12. Nagy, F. & Dickinson, P. S. Control of a central pattern generator by an identified modulatory interneurone in crustacea. I. Modulation of the pyloric motor output. *J. Exp. Biol.* 105, 33–58 (1983).
13. Beltz, B. *et al.* Serotonergic innervation and modulation of the stomatogastric ganglion of three decapod crustaceans (*Homarus americanus*, *Cancer irroratus*, and *Panulirus interruptus*). *J. Exp. Biol.* 109, 35–54 (1984).
14. Eisen, J. S. & Marder, E. A mechanism for production of phase shifts in a pattern generator. *J. Neurophysiol.* 51, 1375–1393 (1984).
15. Hooper, S. L. & Marder, E. Modulation of a central pattern generator by two neuropeptides, proctolin and FMRFamide. *Brain Res.* 305, 186–191 (1984).
16. Flamm, R. E. & Harris-Warrick, R. M. Aminergic modulation in lobster stomatogastric ganglion. I. Effects on motor pattern and activity of neurons within the pyloric circuit. *J. Neurophysiol.* 55, 847–865 (1986).
17. Harris-Warrick, R. M. & Flamm, R. E. Chemical modulation of a small central pattern generator circuit. *Trends Neurosci.* 9, 432–437 (1986).
18. Hooper, S. L. & Marder, E. Modulation of the lobster pyloric rhythm by the peptide, proctolin. *J. Neurosci.* 7, 2097–2112 (1987).
19. Nusbaum, M. P. & Marder, E. A neuronal role for a crustacean red pigment

- concentrating hormone-like peptide: neuromodulation of the pyloric rhythm in the crab, *Cancer borealis*. *J. Exp. Biol.* **135**, 165–181 (1988).
20. Nusbaum, M. P. & Marder, E. A modulatory proctolin-containing neuron (MPN). II. State-dependent modulation of rhythmic motor activity. *J. Neurosci.* **9**, 1600–1607 (1989).
 21. Turrigiano, G. G. & Selverston, A. I. Cholecystokinin-like peptide is a modulator of a crustacean central pattern generator. *J. Neurosci.* **9**, 2486–2501 (1989).
 22. Katz, P. S. & Harris-Warrick, R. M. Actions of identified neuromodulatory neurons in a simple motor system. *Trends Neurosci.* **13**, 367–373 (1990).
 23. Turrigiano, G. G. & Selverston, A. I. A cholecystokinin-like hormone activates a feeding-related neural circuit in lobster. *Nature* **344**, 866–868 (1990).
 24. Harris-Warrick, R. M. & Marder, E. Modulation of neural networks for behavior. *Annu. Rev. Neurosci.* **14**, 39–57 (1991).
 25. Blitz, D. M., Christie, A. E., Marder, E. & Nusbaum, M. P. Distribution and effects of tachykinin-like peptides in the stomatogastric nervous system of the crab, *Cancer borealis*. *J. Comp. Neurol.* **354**, 282–294 (1995).
 26. Norris, B. J., Coleman, M. J. & Nusbaum, M. P. Pyloric motor pattern modification by a newly identified projection neuron in the crab stomatogastric nervous system. *J. Neurophysiol.* **75**, 97–108 (1996).
 27. Hooper, S. L. Phase maintenance in the pyloric pattern of the lobster (*Panulirus interruptus*) stomatogastric ganglion. *J. Computational Neurosci.* **4**, 191–205 (1997).
 28. Hooper, S. L. The pyloric pattern of the lobster (*Panulirus interruptus*) stomatogastric ganglion comprises two phase-maintaining subsets. *J. Computational Neurosci.* **4**, 207–219 (1997).
 29. Selverston, A. I., Russell, D. F., Miller, J. P. & King, D. G. The stomatogastric nervous system: structure and function of a small neural network. *Prog. Neurobiol.* **7**, 215–290 (1976).
 30. Eisen, J. S. & Marder, E. Mechanisms underlying pattern generation in lobster stomatogastric ganglion as determined by selective inactivation of identified neurons III. Synaptic connections of electrically coupled pyloric neurons. *J. Neurophysiol.* **48**, 1392–1415 (1982).
 31. Russell, D. F. & Hartline, D. K. Bursting neural networks: A reexamination. *Science* **200**, 453–456 (1978).
 32. Hartline, D. K. Pattern generation in the lobster (*Panulirus*) stomatogastric ganglion. II. Pyloric network simulation. *Biol. Cybern.* **33**, 223–236 (1979).
 33. Miller, J. P. & Selverston, A. I. Mechanisms underlying pattern generation in lobster stomatogastric ganglion as determined by selective inactivation of identified neurons. II. Oscillatory properties of pyloric neurons. *J. Neurophysiol.* **48**, 1378–1391 (1982).
 34. Hartline, D. K., Gassie, D. V. & Sirchia, C. D. in *The Crustacean Stomatogastric System* (eds Selverston, A. I. & Moulins, M.) 75–77 (Springer, Berlin, 1987).
 35. Golowasch, J. & Marder, E. Ionic currents of the lateral pyloric neuron of the stomatogastric ganglion of the crab. *J. Neurophysiol.* **67**, 318–331 (1992).
 36. Tierney, A. J. & Harris-Warrick, R. M. Physiological role of the transient potassium current in the pyloric circuit of the lobster stomatogastric ganglion. *J. Neurophysiol.* **67**, 599–609 (1992).
 37. Harris-Warrick, R. M., Coniglio, L. M., Barazangi, N., Guckenheimer, J. & Gueron, S. Dopamine modulation of transient potassium current evokes phase shifts in a central pattern generator network. *J. Neurosci.* **15**, 342–358 (1995).
 38. Miller, J. P. & Selverston, A. I. Rapid killing of single neurons by irradiation of intracellularly injected dye. *Science* **206**, 702–704 (1979).
 39. Bidaut, M. Pharmacological dissection of pyloric network of the lobster stomatogastric ganglion using picrotoxin. *J. Neurophysiol.* **44**, 1089–1101 (1980).
 40. Miller, J. P. & Selverston, A. I. Mechanisms underlying pattern generation in lobster stomatogastric ganglion as determined by selective inactivation of identified neurons. IV. Network properties of pyloric system. *J. Neurophysiol.* **48**, 1416–1432 (1982).
 41. LeMasson, G., Marder, E. & Abbott, L. F. Activity-dependent regulation of conductances in model neurons. *Science* **259**, 1915–1917 (1993).
 42. Turrigiano, G., Abbott, L. F. & Marder, E. Activity-dependent changes in the intrinsic properties of cultured neurons. *Science* **264**, 974–977 (1994).
 43. Turrigiano, G., LeMasson, G. & Marder, E. Selective regulation of current densities underlies spontaneous changes in the activity of cultured neurons. *J. Neurosci.* **15**, 3640–3652 (1995).
 44. Marder, E., Abbott, L. F., Turrigiano, G. G., Liu, Z. & Golowasch, J. Memory from the dynamics of intrinsic membrane currents. *Proc. Natl. Acad. Sci. USA* **93**, 13481–13486 (1996).
 45. Maynard, D. M. & Dando, M. R. The structure of the stomatogastric neuromuscular system in *Callinectes sapidus*, *Homarus americanus* and *Panulirus argus* (decapoda crustacea). *Phil. Trans. R. Soc. Lond. B Biol. Sci.* **268**, 161–220 (1974).
 46. Konishi, M., Takahashi, T. T., Wagner, H., Sullivan, W. E. & Carr, C. E. in *Auditory Function: Neurobiological Bases of Hearing* (eds Edelman, G. M., Gall, W. E. & Cowan, W. M.) 721–745 (Wiley, New York, 1988).